

## DISUBSTITUTED 1,2,3-TRIAZOLES AS AMIDE BOND MIMETICS

DOI: <http://dx.medra.org/10.17374/targets.2018.21.1>

Miriam Corredor, Jordi Solà and Ignacio Alfonso\*

Department of Biological Chemistry and Molecular Modelling, IQAC-CSIC

Jordi Girona 18-26, 08034 Barcelona, Spain

(e-mail: [ignacio.alfonso@iqac.csic.es](mailto:ignacio.alfonso@iqac.csic.es))

**Abstract.** Disubstituted 1,2,3-triazole rings represent a family of very unique aromatic heterocycles with interesting properties that make them excellent mimetics of amide bonds. Thus, their polarity and H-bond abilities, as well as their geometrical properties have led to the replacement of amide bonds by differently substituted 1,2,3-triazoles in peptides and peptidomimetics. This chapter contains an introductory view to the topic as well as selected representative examples of the most recent research in the field.

### Contents

1. Introduction
  2. Synthesis of disubstituted 1,2,3-triazole rings
    - 2.1. Synthesis of 1,4-disubstituted-1,2,3-triazoles
    - 2.2. Synthesis of 1,5-disubstituted-1,2,3-triazoles
    - 2.3. Synthesis of 2,4-disubstituted-1,2,3-triazoles
  3. Structural properties
    - 3.1. Physico-chemical properties of the differently substituted 1,2,3-triazoles
    - 3.2. Structural characterization
  4. Disubstituted triazole rings in peptides
    - 4.1. Triazole as a peptide bond mimic
    - 4.2. Cyclic peptides
    - 4.3. Oligomeric triazolamers
  5. Disubstituted triazole rings in peptoids
  6. Conclusions
- Acknowledgements  
References

### 1. Introduction

The triazole ring is a five-membered aromatic heterocycle that contains three nitrogen and two carbon atoms.<sup>1</sup> Accordingly, it can present two different isomers depending on the relative disposition of the nitrogen atoms: 1,2,3-triazole<sup>2</sup> and 1,2,4-triazole.<sup>3</sup> Moreover, each of the isomers can exist as different tautomers depending on the position of the hydrogen attached to the nitrogen (Figure 1).<sup>1</sup> Some of the tautomers can be equivalent by symmetry depending on the corresponding substitution.

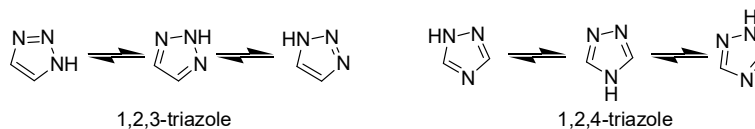


**Figure 1.** Different isomeric structures of the triazole heterocyclic ring.

This heterocycle is present in different natural products and synthetic compounds used as antifungal drugs or in the agriculture and food industries.<sup>4</sup> The different substitution in the triazole leads to differences in the chemical and biological properties of the heterocycle. In this chapter, we will focus on the 1,2,3-triazole ring for two main reasons. First of all, the recently developed synthetic methods used for the easy and selective synthesis of disubstituted 1,2,3-triazole rings have enormously increased its applications in different areas of chemistry. On the other hand, this substitution pattern produces a heterocycle that shares structural and physicochemical properties with the amide bond, which is a key functional group in organic

chemistry and, specially, chemical biology. The combination of this two facts has made the disubstituted 1,2,3-triazole a pivotal heterocycle in chemistry and for the development of technological applications, bioconjugation procedures and biomimetic drugs.<sup>5</sup> In this chapter, we do not intend to make an exhaustive review of the many different synthetic approaches and specific applications of this moiety, but to give a general and introductory view of the potential of this heterocycle in different fields of chemistry, especially when used as amide bond surrogate in peptides and peptidomimetics.<sup>6</sup>

## 2. Synthesis of disubstituted 1,2,3-triazole rings

Considering disubstituted triazoles, there are three isomers with different possibilities in the position of the residues attached to the heterocyclic ring. Those are 1,4-, 1,5- and 2,4-disubstituted triazoles. The structural and electronic properties of the three isomers are obviously different, as it will be highlighted below. In this section, the main synthetic approaches toward these functionalities will be briefly discussed.

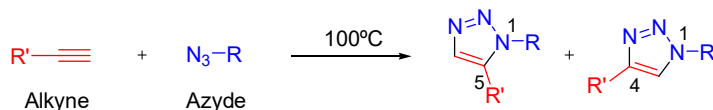
### 2.1. Synthesis of 1,4-disubstituted-1,2,3-triazoles

The synthesis of this heterocycle has exploded in the last years after the development of the click chemistry approaches to its preparation. Click chemistry is a term that was introduced by K. B. Sharpless in 2001 to describe reactions that fulfil a set of criteria.<sup>7</sup> The reaction must be modular, wide in scope, render very high yields, generate only non-toxic by-products that can be removed by non-chromatographic methods, and be stereospecific. The required characteristics include simple reaction conditions, readily available starting materials, the use of no solvent or a solvent that is benign or easily removed, and simple product isolation. It is important to recognize that click reactions achieve their required characteristics by having a high thermodynamic driving force, usually higher than 20 kcal/mol.

Applications of click chemistry are increasingly found in all aspects of drug discovery;<sup>5</sup> they range from lead finding through combinatorial chemistry and target-template *in vitro* chemistry, to proteomics and DNA research. Click chemistry features are beautifully represented among cycloaddition reactions involving heteroatoms, such as hetero-Diels-Alder and, particularly, 1,3-dipolar cycloadditions. These modular fusion reactions connect two unsaturated reactants and provide fast access to a wide variety of interesting five- and six-membered heterocycles. Among these reactions<sup>8</sup> the Huisgen dipolar cycloaddition is the most useful and reliable.

Huisgen's dipolar cycloaddition<sup>9</sup> of organic azides and alkynes is the most direct route to 1,2,3-triazoles. In the absence of a transition-metal catalyst, these reactions are not regioselective, relatively slow and require high temperatures and long reaction times to reach acceptable yields.<sup>10</sup>

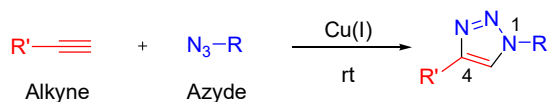
Due to the fact that the reaction is highly exothermic (*ca.* -50 to 65 kcal/mol), its high activation barrier (25-26 kcal/mol for methyl azide and propyne)<sup>11</sup> results in exceedingly low reaction rates for inactivated reactants even at elevated temperature. Furthermore, since the difference in HOMO-LUMO energy levels for both azides and alkynes are of similar magnitude, both dipole-HOMO and dipole-LUMO controlled pathways operate in these cycloadditions. As a result, a mixture of regioisomeric 1,2,3-triazole products is usually formed when an alkyne is asymmetrically substituted (Scheme 1).<sup>12</sup>



**Scheme 1.** Huisgen dipolar cycloaddition reaction.

Copper (I) catalysis discovered independently by the groups of Meldal<sup>13</sup> and Sharpless<sup>7</sup> accelerates the reaction to minutes and at much lower temperatures. The result of this copper catalysed reaction is mostly, if not completely, a 1,4-triazole adduct (Scheme 2). The copper catalysed reaction proceeds in both aqueous and organic solvents under simple experimental conditions. These features along with the unnecessary requirement of high temperatures makes this copper catalysed azide-alkyne cycloaddition (CuAAC) a useful

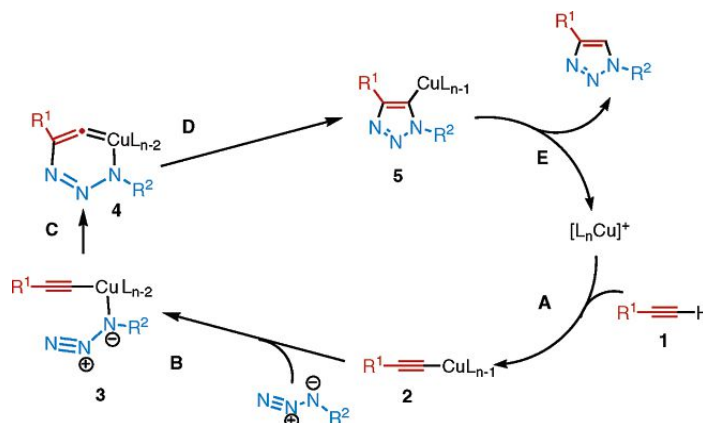
tool for synthetic chemists.<sup>14</sup> Moreover, the cycloaddition is thermodynamically favourable enough to be irreversible.



**Scheme 2.** Copper-catalysed Azide-Alkyne Cycloaddition (CuAAC).

While a number of copper (I) sources can be directly used, it was found that the catalyst is better prepared *in situ* by reduction of Cu(II) salts, which are less costly and often purer than Cu(I) salts. As reducing agent, ascorbic acid and/or sodium ascorbate proved to be excellent for the preparation of a broad spectrum of 1,4-disubstituted-1,2,3-triazole products in high yields and purities at 0.25-2 mol% catalyst loading.<sup>14</sup>

The mechanism proposed for the CuAAC (Scheme 3) begins with the formation of copper (I) acetylide, after which the azide displaces another ligand and binds to the metal. Then, an unusual six-membered copper (III) metallacycle is formed. The barrier for this process has been calculated to be considerably lower than the one for the uncatalysed reaction. Ring contraction to a triazolyl-copper derivative is followed by protonolysis that delivers the triazole product and closes the catalytic cycle.<sup>11</sup>



**Scheme 3.** Mechanism proposed for the CuAAC.

As it has been shown, the copper-catalysed 1,3-dipolar azide-alkyne cycloaddition (CuAAC) was an important advance in the chemistry of 1,2,3-triazoles. A significant rate acceleration ( $10^7$  to  $10^8$  compared to the non-catalysed process), a remarkably broad scope, a tolerance to aqueous and oxidative conditions, and an exclusive regioselectivity have enabled a number of applications in the relatively short time since the reaction was discovered. Examples of these applications are found in: drug discovery,<sup>15</sup> bioconjugations,<sup>16</sup> polymer and material science<sup>17</sup> and related areas<sup>18</sup> including supramolecular chemistry.<sup>19</sup>

## 2.2. Synthesis of 1,5-disubstituted-1,2,3-triazoles.

While Cu(I) catalysis provides reliable means for the assembly of 1,4-disubstituted-1,2,3-triazoles, a general method for the generation of the 1,5-disubstituted regioisomers was lacking. Although they can be synthesized by the reaction of bromomagnesium acetylides with organic azides,<sup>20</sup> this procedure lacks the scope and convenience of the CuAAC process.

In fact, 1,5-isomers have been only scarcely explored so far,<sup>21</sup> although Fokin and co-workers<sup>22</sup> reported that their preparation can be accomplished by a ruthenium-catalysed azide-alkyne cycloaddition

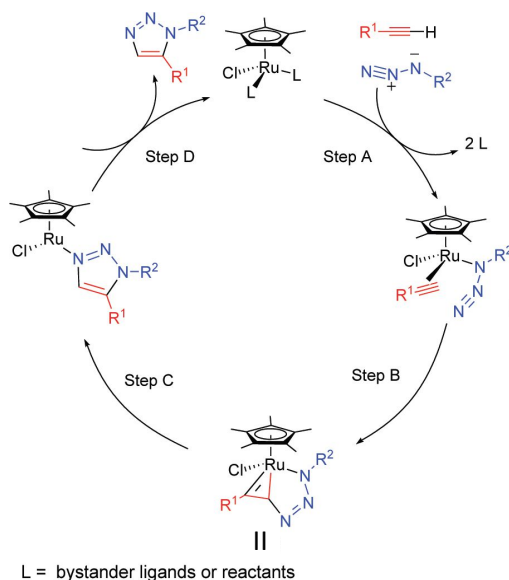
reaction (RuAAC). This reaction furnishes the triazole derivatives with a virtually total 1,5-regioselectivity.<sup>22</sup>

Catalytic transformations of alkynes mediated by ruthenium complexes were well-known. Therefore, ruthenium was a logical choice on the research for a catalyst of azide-alkyne cycloaddition. Different ruthenium complexes were tested by Jia, Fokin and co-workers.<sup>22</sup> Acetate complex,  $\text{RuCl}_2(\text{PPh}_3)_3$  or  $\text{RuHCl}(\text{CO})(\text{PPh}_3)_3$  were ineffective. In contrast,  $\text{Cp}^*\text{RuCl}(\text{PPh}_3)_2$  catalyst resulted in 50% conversion of the reactants to a mixture of 1,5- and 1,4-disubstituted triazoles. Then, a simple switch to the pentamethyl analogue,  $\text{Cp}^*\text{RuCl}(\text{PPh}_3)_2$ , resulted in the exclusive formation of 1,5-regioisomer with complete conversion. Reactions with other  $[\text{Cp}^*\text{Ru}]$  complexes gave similar results.<sup>22,23</sup>

The scope of the reaction was also studied and the fact that it is not very sensitive to the alkyne but to the nature of the azide was proved. Primary azides were more efficient than secondary ones, while tertiary azides reluctantly participated in the catalysis. These cycloadditions proceed well in aprotic organic solvents (benzene, toluene, THF, dioxane) whereas protic solvents have a detrimental effect on both the yield and the regioselectivity.

Since Cu (I) acetylides seem to be the intermediates in the CuAAC, this transformation is limited to terminal alkynes. On the contrary, the  $[\text{Cp}^*\text{RuCl}]$  system is active with internal alkynes as well,<sup>24</sup> which suggests that ruthenium acetylides are not involved in the catalytic cycle. It was proposed that the neutral  $[\text{Cp}^*\text{RuCl}]$  is the catalytically active species and the following mechanism was suggested.<sup>12,22</sup>

The displacement of the spectator ligands (step A in Scheme 4) produces the activated complex **I**, which is converted, via the oxidative coupling of an alkyne and an azide (step B), to the ruthenacycle **II**. This step controls the observed 1,5-regioselectivity. The new C-N bond is formed between the most electronegative and less sterically demanding carbon of the alkyne and the terminal nitrogen of the azide. The metallacycle intermediate then undergoes reductive elimination (step C) releasing the aromatic triazole product and regenerating the catalyst (step D) or the activated complex **I**.

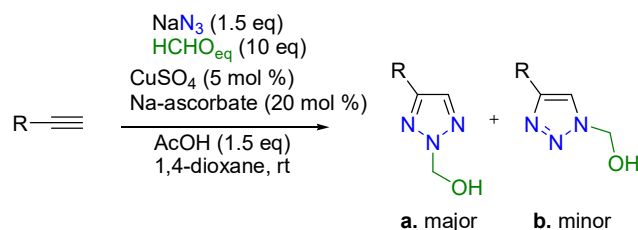


**Scheme 4.** Proposed intermediates in the catalytic cycle of RuAAC reaction.

### 2.3. Synthesis of 2,4-disubstituted-1,2,3-triazoles.

Regarding the third possible disubstituted isomer of the 1,2,3-triazole, although the 2-substituted-2*H*-1,2,3-triazoles can be obtained by alkylation of *NH*-1,2,3-triazoles with the suitable electrophilic reagents, a mixture of the isomeric products is often produced. Other possibilities are the oxidative cyclization of

bishydrazones or bissemicarbazones<sup>25</sup> and the three-component Pd-catalysed reaction that form 2-allyl-1,2,3-triazoles.<sup>26</sup> Despite these reports, a general and simple method for the stereoselective formation of the 2*H*-isomers is still not available. In 2008, Fokin and co-workers reported a three-component one-pot synthesis of 2-hydroxymethyl-2*H*-1,2,3-triazoles.<sup>27</sup> As shown in Scheme 5, the reaction afforded a mixture of two compounds.



**Scheme 5.** Synthesis of *N*-hydroxymethyl-1,2,3-triazoles.

These compounds are versatile intermediates that can be used for the preparation of *NH*-1,2,3-triazoles. In their method, formaldehyde, sodium azide and a terminal alkyne react in a one-pot two-steps process under acidic conditions. Azidomethanol, formed *in situ* from protonated formaldehyde and sodium azide, is a likely intermediate. The subsequent copper (I)-catalysed reaction with the alkyne provides the 1-hydroxymethyl-1*H*-1,2,3-triazole product. However, the instability of this derivative and its equilibrium with the *NH*-triazole and formaldehyde results in the rearrangement of the 1-hydroxymethyl triazole to the thermodynamically more stable 2-hydroxymethyl isomer. Thus, a mixture of the 1-hydroxymethyl-1,2,3-triazole (**b**) and the 2-hydroxymethyl (**a**) isomers is obtained, being the desired isomer (**a**) the major and the most stable one (Scheme 5).

### 3. Structural properties of disubstituted 1,2,3-triazole rings

#### 3.1. Physico-chemical properties of the differently substituted 1,2,3-triazoles

The triazole ring has an aromatic planar conformation with very remarkable structural properties. The optimized geometries using DFT (B3LYP/6-31+G\*) for the three different substitution patterns (with two methyl residues as model compounds) are depicted in Figure 2.

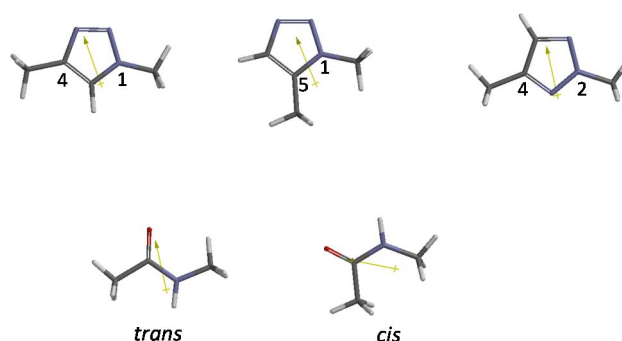


**Figure 2.** DFT optimized structures for dimethyl disubstituted 1,2,3-triazole isomeric rings and *trans/cis*-*N*-methylacetamide. The figure also shows the calculated dipolar moment.

The corresponding structures for a model amide (*N*-methyl acetamide) in the *trans* and *cis* conformations are also shown. The figure also shows the calculated dipolar moments, while their corresponding values (debyes) along with the methyl-methyl C-C distances are displayed in Table 1 for the

suitable comparison. From the data shown in Figure 2 and Table 1, one can conclude that the 1,4-disubstituted triazole should be a very good *trans*-amide surrogate with very similar polarity, while showing a slightly longer C-C distance (entries 1 and 3 in Table 1). On the contrary, the 1,5-derivative is geometrically very similar to the amide bond in a *cis* conformation, despite the polarity is rather different, mainly in terms of the orientation of the dipole moment (entries 2 and 4 in Table 1). Additionally, the CH bond in the triazole rings is highly polarized, being a good hydrogen bond donor. On the other hand, the electron pairs of the nitrogen atoms of the ring are good hydrogen bond acceptors, making the triazole groups a good mimetic of secondary amides in terms of non-covalent polar interactions (H-bonding donor/acceptor abilities).

**Table 1.** Geometrical properties of model *cis/trans* amide functions and disubstituted 1,2,3-triazole rings, calculated by DFT methods.

entry	structure	Dipolar moment (debyes)	C-C distance (Å)
1	<i>trans</i> amide	3.70	3.816
2	<i>cis</i> amide	3.91	2.929
3	1,4-triazole	4.31	5.045
4	1,5-triazole	5.06	3.148
5	2,4-triazole	0.35	4.877

Finally, the 2,4-disubstituted triazole displays the most distinct structure both in terms of polarity and C-C distance. Thus, this isomer is much less polar than the other triazoles and locates the residues at intermediate distance and angle, with a linear disposition of the substituents. Thus, the 2,4-disubstituted ring can be considered a structural intermediate between the two extreme dispositions and bearing an innocent functionality in terms of polarity of the triazole group.

### 3.2. Structural characterization

As already mentioned, the 1,3-dipolar cycloaddition of organic azides and alkynes is a direct route to 1,2,3-triazoles, but the reaction course is slow and not regioselective. However, the discovery of the catalytic azide-alkyne cycloadditions (using CuAAC or RuAAC, section 2 of this chapter) provides access to the synthesis of 1,2,3-triazoles under mild conditions and excellent regioselectivity.

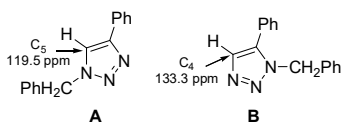
However, the tautomerism and isomerism of triazoles make the structural analysis of these compounds troublesome. The structures of many of these triazoles were elucidated by X-ray crystallography analysis,<sup>28</sup> or by sophisticated NMR methods, including NOE,<sup>29</sup> HMQC, HSQC and HMBC studies.<sup>30</sup>

While the structures of triazoles prepared by the Sharpless/Fokin research groups and in other studies have been rigorously demonstrated,<sup>31</sup> in many subsequent examples the structures of the isolated triazoles are not proved but simply assigned using the assumption that Cu(I) catalysis gives 1,4-disubstituted isomers, while Ru (II) catalysis gives the 1,5- distribution. In any case, when a mixture of the two or three possible 1,2,3-triazole isomers is obtained, a reliable method for the verification of the structure is necessary.

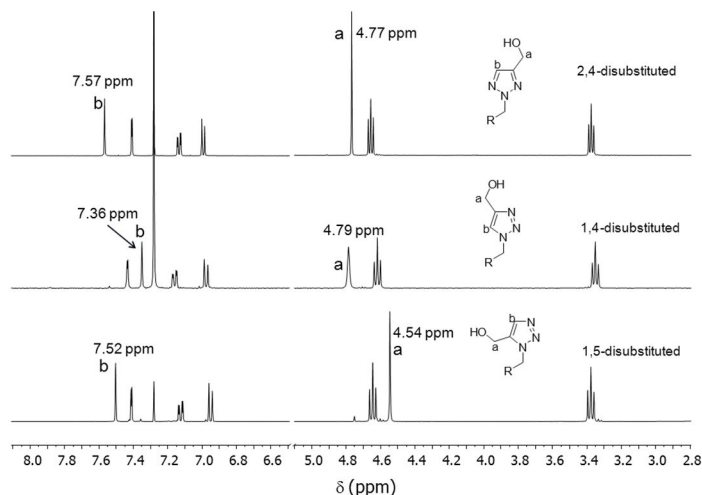
Creary *et al.*<sup>32</sup> recently reported a simple method combining <sup>13</sup>C NMR and computational observations for distinguishing between 1,4- and 1,5-disubstituted 1,2,3-triazoles. As shown in Figure 3, each isomer has a different <sup>13</sup>C NMR chemical shift. For the 1,4-disubstituted-triazole (**A**), the CH signal appears at ~120 ppm for C5, while C4 in **B** is at ~133 ppm. These <sup>13</sup>C NMR signals are readily identified by the large <sup>1</sup>J<sub>CH</sub> coupling constants in the gated decoupled <sup>13</sup>C NMR spectrum. These authors also demonstrated that B3LYP/6-31G\* GIAO computational studies agree with this trend, although calculated shifts are consistently about 6 ppm upfield from the experimental values.

However, this assignment showed troublesome for the 2,4-disubstituted counterpart, since it shows chemical environments that are hybrid between the two other isomers. This is illustrated in Figure 4 for the

$^1\text{H}$  NMR spectra of the different isomers bearing equivalent substituents ( $\text{R}_1 = \text{CH}_2\text{OH}$  and  $\text{R} = 2,4$ -dichlorobenzyl).



**Figure 3.** Characteristic  $^{13}\text{C}$  signal to distinguish between 1,4- (**A**) and 1,5- (**B**) disubstituted triazoles.

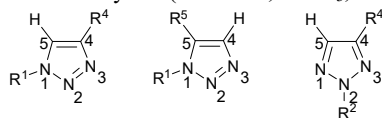


**Figure 4.**  $^1\text{H}$  NMR spectra of representative 1,5-, 1,4- or 2,4-disubstituted 1,2,3-triazole, respectively.

The triazole proton (**b**) is slightly different depending on the isomer, being more shielded in the 1,4-isomer (7.36 ppm) than for the other isomers (7.52 and 7.57 ppm for 1,5- and 2,4-isomers, respectively). The same trend was observed when  $\text{R}^1$  was the aldehyde moiety (Table 2), appearing at the lowest chemical shift the proton **a** of the 1,4-disubstituted isomer (7.89 ppm) whereas for the other one, it appeared over 8 ppm. This tendency was observed generally with a wide range of substituents (Table 2).

Thus, the triazole proton chemical shifts serves to distinguish the 1,4-isomer from the other ones, while the  $\text{CH}_2$  of the hydroxymethyl group signal allows to distinguish the 1,5-isomer. In this isomer, the proton **a** appeared at the lowest chemical shift (4.54 ppm) but at around 4.78 ppm in the other substitution patterns, which is a remarkable difference. The same effect was observed with other  $\text{R}^2$  (Table 2). For the case of the benzyl group, the proton **a** showed a chemical shift of 4.63 ppm in the 1,5-isomer, whereas in the 1,4- and 2,4-substituted ring the value was higher (4.79 and 4.77, respectively). In the *p*-fluorophenethyl derivative, the difference is even higher, being the chemical shift 4.41 ppm for 1,5-substitution and 4.77 for the 1,4 and 2,4-isomers.

On the other hand, as reported in the article of Creary *et al.*,<sup>32</sup> the CH carbon of the triazole can be used to identify which of the two isomers (1,4- or 1,5-disubstituted) is formed.<sup>32</sup> However, the comparison of a wider family of molecules including 2,4-disubstituted isomers showed ambiguous data (Table 2). For a more general assignment of the isomers, a complete structural characterization of different 1,2,3-triazoles bearing different di-substitution patterns has been recently carried out.<sup>33</sup> In this study, the authors included the data corresponding to the  $^{15}\text{N}$  NMR chemical shift, obtained by  $^1\text{H}$ - $^{15}\text{N}$  HMBC correlation experiments. The  $^1\text{H}$ ,  $^{13}\text{C}$  and  $^{15}\text{N}$  NMR chemical shift data are reported in Table 2.

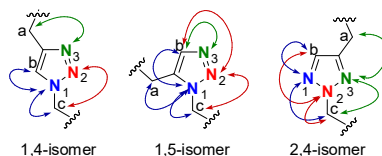
**Table 2.** Experimental  $^{15}\text{N}$ ,  $^{13}\text{C}$  and  $^1\text{H}$  chemical shifts (ppm) for the corresponding nuclei in the isomeric triazole heterocycles (400 MHz,  $\text{CDCl}_3$ , 298 K).

Subs. <sup>a</sup>	R <sup>1,b</sup>	R <sup>2,b</sup>	R <sup>4</sup>	R <sup>5</sup>	N <sup>1</sup>	N <sup>2</sup>	N <sup>3</sup>	C <sup>4</sup>	C <sup>5</sup>	CH <sup>c</sup>
1,4-	DCP	-	CH <sub>2</sub> OH	-	-134.8	-18.3	-31.5	147.9	122.1	7.36
1,4-	Bn	-	CH <sub>2</sub> OH	-	-133.7	-19.4	-37.2	147.7	121.8	7.46
1,4-	pFP	-	CH <sub>2</sub> OH	-	-134.4	-19.9	-36.1	147.5	122.2	7.34
1,4-	DCP	-	CHO	-	-130.9	-12.8	-18.9	146.6	125.7	7.89
1,4-	Bn	-	CHO	-	-126.4	-11.6	-20.9	148.0	125.0	8.00
1,4-	pFP	-	CHO	-	-130.1	-12.7	-19.6	147.5	125.4	7.80
1,4-	DCP	-	Ph	-	-134.4	-18.2	-34.4	147.6	119.8	7.53
1,5-	DCP	-	-	CH <sub>2</sub> OH	-144.1	-22.9	-40.9	132.9	136.5	7.52
1,5-	Bn	-	-	CH <sub>2</sub> OH	-135.4	-13.8	-33.4	133.5	135.6	7.58
1,5-	pFP	-	-	CH <sub>2</sub> OH	-136.1	-16.6	-35.3	132.5	136.4	7.42
1,5-	DCP	-	-	CHO	-142.4	-9.3	-38.6	141.1	133.9	8.23
1,5-	Bn	-	-	CHO	-132.4	-2.1	-31.7	141.1	133.3	8.25
2,4-	-	DCP	CH <sub>2</sub> OH	-	-50.1	-126.7	-55.9	147.8	132.5	7.57
2,4-	-	Bn	CH <sub>2</sub> OH	-	-49.5	-124.8	-55.9	148.0	132.9	7.61
2,4-	-	pFP	CH <sub>2</sub> OH	-	-51.5	-127.5	-57.6	147.5	132.4	7.57
2,4-	-	DCP	CHO	-	-41.4	-119.0	-47.4	146.9	135.1	8.07
2,4-	-	pFP	CHO	-	-41.9	-119.7	-48.8	147.0	134.6	8.04

<sup>a</sup>Subs: substitution pattern of the triazole rings; <sup>b</sup>DCP: 2,4-dichlorophenethyl; pFP: *para*-fluorophenethyl; <sup>c</sup>CH: refers to the triazole proton, being H<sup>5</sup> for the 1,4- and 2,4-disubstituted 1,2,3-triazole but H<sup>4</sup> for the 1,5-isomer.

It is clear that the  $^{13}\text{C}$  chemical shift of the CH in the 1,5-isomer (~132 ppm) appears around 10 ppm higher than the same carbon in the 1,4-isomer (~122 ppm). Whereas the quaternary carbon shows the opposite tendency because the chemical shift of the 1,4-isomer is around 147 ppm and the one for the 1,5-isomer resonates at ~137 ppm. Therefore, by using the  $^{13}\text{C}$  NMR technique, it is possible to unambiguously assign the appropriate isomer between 1,4- and 1,5-substituted triazole. However, this method is not useful for the 2,4-isomer, because the substituted carbon has a similar chemical shift to that of the 1,4-isomer and the CH carbon is similar to that of the 1,5-isomer. This effect is similarly observed in the  $^1\text{H}$  NMR, where the 2,4-isomer is a kind of combination of the other ones.

Having in mind these difficulties to assign the triazoles isomers, the  $^1\text{H}$ - $^{15}\text{N}$  HMBC experiments have been compared to differentiate the substitution patterns. The  $^1\text{H}$ - $^{15}\text{N}$  correlations of the three different isomers are shown in Figure 5.

**Figure 5.** Peak correlations found in the  $^1\text{H}$ - $^{15}\text{N}$  HMBC spectra for the disubstituted triazole derivatives.

For each isomer, the nitrogen that appears at the lowest chemical shift (less than -100 ppm, using nitromethane as the chemical shift reference for  $^{15}\text{N}$ ) is the alkylated one, being N<sup>1</sup> in **I** and **II** and N<sup>2</sup> in **III**. Besides, N<sup>1</sup> of 1,5-isomer (**II**) shows correlation peaks with protons **a**, **b** and **c** at the same time, which is



impossible in both 1,4- and 2,4-isomers because the alkylated nitrogen ( $N^1$  and  $N^2$  respectively) is too far from the proton **a** in both cases. In the 2,4-isomer (**III**),  $N^3$  has correlation peaks with protons **a** and **c**. This is not possible in the 1,4-isomer (**I**), because  $N^3$  in this isomer is too far from the proton **c** to show a correlation peak. Likewise  $N^2$  in the 1,4-isomer, which correlates with proton **c**, is too far from **a**. Therefore, the two simultaneous correlations are only possible for the 2,4-isomer.

For a better illustration of the utility of the bidimensional  $^1\text{H}$ - $^{15}\text{N}$  correlation spectra, in the following picture, a comparison of the  $^1\text{H}$ - $^{15}\text{N}$  HMBC of the three isomers with the 2,4-dichlorophenethyl substituent is represented and the differences already explained are depicted (Figure 6).

Finally, the chemical shifts have been also predicted by GIAO DFT theoretical calculations, showing a very good empirical correlation with the experimental chemical shifts.<sup>33</sup> Thus, the  $^{15}\text{N}$  NMR chemical shifts have proved to be the definitive tool for the unambiguous characterization of the substitution patterns in the 1,2,3-triazole heteroaromatic ring.

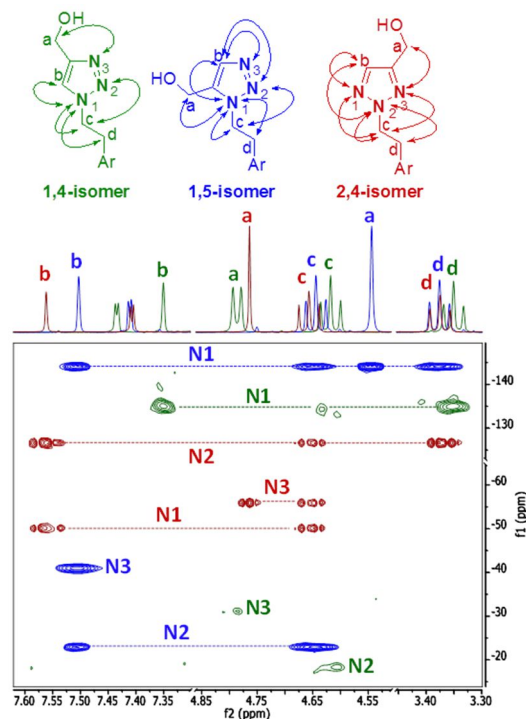


**Figure 6.** Comparison of the  $^1\text{H}$ - $^{15}\text{N}$  HMBC of the 1,4-, 1,5- and 2,4-isomers being Ar = 2,4-dichlorophenyl.

## 4. Disubstituted triazole rings in peptides

### 4.1. Triazole as a peptide bond mimic

Given the biological importance of peptides and their potential therapeutic properties a lot of effort has been put in the development of molecules that contain a peptidic bond surrogate to replace the enzymatically labile amide function and, consequently, increase their metabolic stability.<sup>6</sup> In this context, disubstituted-1,2,3-triazoles provide a unique platform due to its similarity to the structure of the amide bonds in terms of planarity, size, hydrogen bond properties and dipole moment (Section 3.1). Importantly, the triazole linkage is resistant to enzymatic degradation, oxidation and hydrolysis and therefore is an attractive structure to replace the peptidic bond in biologically active compounds.<sup>34</sup> The acidity of the C-H bond allows establishing hydrogen-bond contacts with appropriate acceptors while the  $N^2$  and  $N^3$  can act as hydrogen-bond acceptors.

In addition, the important dipolar moment of the triazole offers the possibility to establish electrostatic interactions with other dipoles (such as the amide bond) to provide regular secondary structures. While 1,4-disubstituted-1,2,3-triazoles can be considered isosteres of the *trans* amide bond and their use is widespread, 1,5-disubstituted-1,2,3-triazoles are geometrically analogous to the *cis*-amide bond<sup>21a,35</sup> despite its use in peptidomimetics is much less common. Not surprisingly the incorporation of a 1,5-disubstituted triazole into a peptidic chain favours the formation of a turn in the secondary structure (Figure 7).

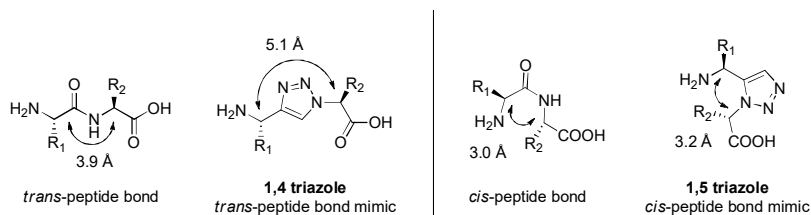
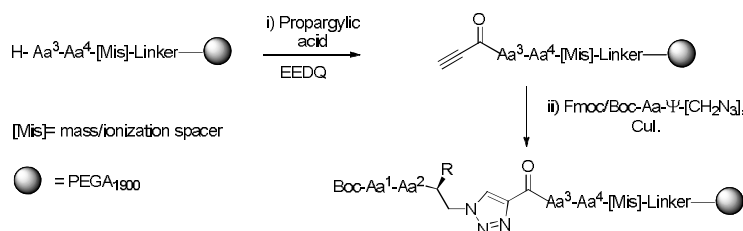


**Figure 7.** Structural similarities between amide bond and 1,4-disubstituted-1,2,3-triazoles.

The introduction of a 1,4-disubstituted-1,2,3-triazole as a peptide bond surrogate was pioneered by the groups of Meldal and Ghadiri. Meldal first used the CuAAC copper(I)-catalysed 1,3-dipolar cycloaddition of terminal alkynes to azides in solid support to couple small peptides either through the main backbone or through amino acid side-chains.<sup>13</sup> The Azide-Alkyne Huisgen Cycloaddition is compatible with standard protecting groups used in conventional peptide chemistry such as *t*Bu, Boc, Trt or Fmoc. Thus, Meldal's group showed that solid-supported peptides could react with azides in high yields to generate a library of compounds with potential biological activity.<sup>36</sup> Likewise, the group of Fan demonstrated that solid supported peptides can undergo multiple cycles of triazole formation efficiently to generate peptidomimetics with triazole-mixed backbones.<sup>37</sup>

Ghadiri also incorporated the triazole unit first into cyclic peptidomimetics (*vide infra*)<sup>38</sup> and later into  $\alpha$ -helix coiled-coiled peptides.<sup>39</sup> In the latter, circular dichroism studies indicated that the modified peptides largely retained the helical structure; however, depending on the position of the substitution, the thermodynamic stability can be affected (Scheme 7).

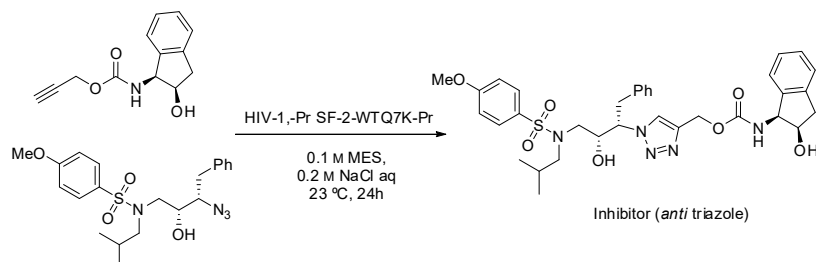


**Scheme 7.** Meldal's synthesis of peptide libraries using a triazole linker.

Several groups have taken advantage of the stability of triazoles to replace the less stable amide group in biologically active compounds. Wlodaver and Wong used this linkage to generate a series of HIV-1 protease inhibitors based on the amprenavir structure.<sup>40</sup> Interestingly, Sharpless, Fokin and Elder reported that an *in situ* click reaction could be employed to generate HIV-1-Pr inhibitors.<sup>41</sup> Remarkably, the authors described that the protease is able to act as template for the formation of its own inhibitor increasing the rate of formation of the *anti* product in the absence of copper (Scheme 8).

More recently, Buntkowsky, Tietze, and Avrutina demonstrated that 1,4- and 1,5-disubstituted 1,2,3-triazoles are valid amide surrogates for the generation of locked *trans* or *cis* conformations that retain biological activity of those peptidomimetics resembling native amide isomers.<sup>42</sup> The group of Mindt also reported that the enhanced proteolytic stability that triazole unit confers to the peptidic backbone generates

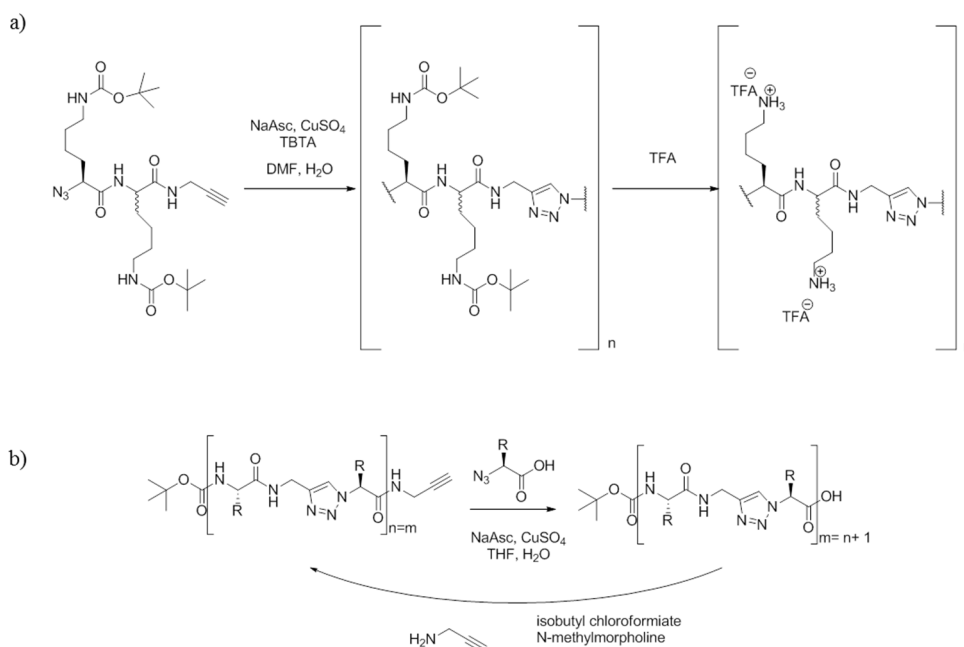
mimetics with improved tumour-targeting capabilities respect to the original peptides as the receptor affinity and cell-internalization properties are maintained.<sup>43</sup>



**Scheme 8.** Synthesis of a HIV-1 protease inhibitor by click chemistry templated by the protease.

Peptidomimetics that contain multiple triazole units in mixed oligopeptides have been described by different synthetic methods. Hecht used the click reaction in a polymerization process to generate polypseudopeptides which yielded different conformations depending on the pH.<sup>44</sup> The polymerization process generated polymers with broad polydispersities ( $1.5 < PDI < 7.8$ ) and molecular weights between 19000 and 180000 g/mol (Scheme 9a).

A different synthetic approach was taken by the group of Chow who reported an iterative procedure to afford linear triazole-based oligopeptides (Scheme 9b).<sup>45</sup> Interestingly, these compounds dimerize in a head-to-tail fashion in non-polar solvents to generate aggregates similar to the antiparallel  $\beta$ -sheets formed by natural peptides.



**Scheme 9.** a) Formation of triazole peptidic polymers by click polymerization described by Hecht.  
b) Preparation of triazole/peptide hybrid oligomers by iterative synthesis described by Chow.

Peptidomimetics combining the amide functionality and 1,5-disubstituted-1,2,3-triazoles have also been explored. For example the group of Beke-Somfai synthesised a series of oligomers of a  $\delta$ -amino acid derivative that contained a 1,5-disubstituted triazole prepared by the RuAAC reaction. The oligomer was conveniently protected as a methyl ester and Boc-carbamate. Thus the elongation strategy was clearly different: the oligomerization proceeded by iterative amide bond formation after the conventional orthogonal deprotection steps. NMR and computational studies suggested that these oligomers adopt several conformations with comparable stabilities.<sup>46</sup> The same group analysed the conformational properties of 1,4- and 1,5-disubstituted 1,2,3-triazole amino acids and their ability to adopt folded structures using a combination of NMR and computational methods.<sup>47</sup> In agreement with experimental results, the authors concluded that 1,4-disubstituted triazoles have a limited number of available conformations, that can lead to extended or bent conformations. In contrast, 1,5-disubstituted compounds present a much higher variety of accessible conformations, thus turn, helix and zig-zag secondary structures probably coexist in solution.

#### 4.2. Cyclic peptides

The great selectivity of the CuAAC reaction allows the facile formation of macrocycles and therefore provides a powerful tool for the synthesis of cyclic peptides (Figure 8).<sup>48</sup>

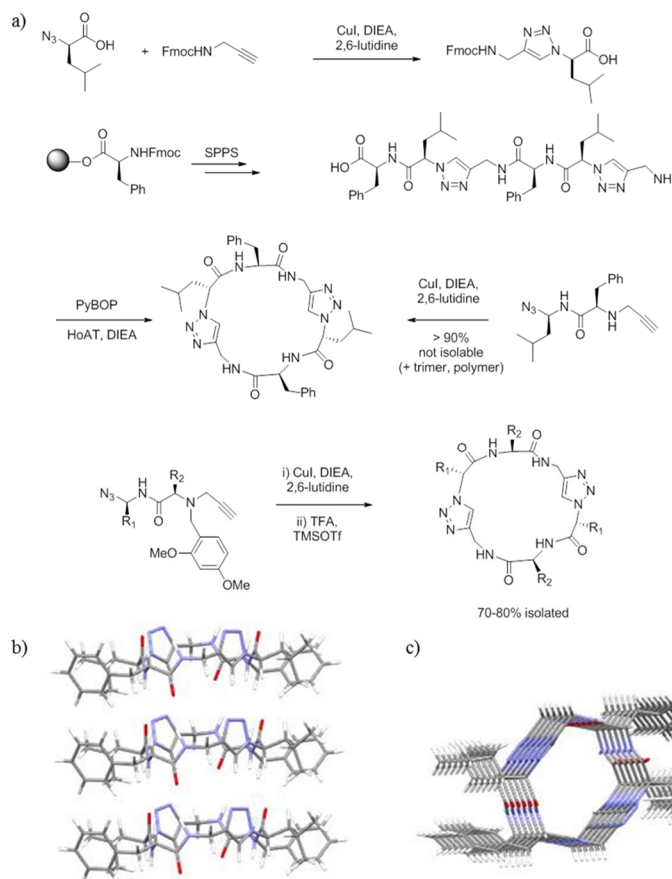


**Figure 8.** Ghadiri's formation of nanotubes containing 1,4-disubstituted triazoles. a) Synthesis of the cyclic pseudopeptides. b) X-ray structure of a nanotube viewed from the side showing the stacking. c) Tilted top view of the nanotube.

As mentioned above the Ghadiri's group was pioneer in the introduction of triazoles into cyclic peptide scaffolds.<sup>48a</sup> To construct cyclic peptidomimetics, a *N*-Fmoc-protected  $\epsilon$ -amino acid containing the triazole linkage was employed in solid-phase peptide synthesis to afford the cyclic structures after a macrolactamization step (Figure 8a). These heterocyclic pseudo-peptide compound form a flat ring structure that allow the formation of nanotubes held together by a network of intermolecular amide backbone hydrogen bonds (Figure 8b,c). This kind of compounds could also be prepared by a 2+2 cyclization with higher yields (> 90%) but their insolubility prevented purification from trimer macrocycles and oligomers. However amide functionalization using Dmb allowed purification by preparative HPLC, providing, after deprotection, the desired cyclic pseudopeptides.<sup>48b</sup>

Other scaffolds have been used for the formation of nanotubes; Chattopadhyay used peptidomimetic macrocycles consisting of a *cis*- $\beta$ -furanoid sugar, a  $\beta$ -alanine and a triazole moiety that assemble in the mentioned structures.<sup>49</sup> Depending on the different orientation of the groups a control of the polarity of the nanotube is possible.<sup>49b</sup> The same group also investigated the substitution of the  $\alpha$ -amino acid by a  $\beta$ -amino acid in the structure but the latter did not self-assemble.<sup>49c</sup> Head-to-tail cyclodimerization of resin-bound peptides can also be accomplished by the Huisgen cycloaddition. Finn reported that the cyclodimerization is achieved in solid-phase but not with the free peptides.<sup>50</sup> Moreover, the number of residues and the properties of the reaction solvents and resin used are critical in order to obtain the cyclic dimer or the corresponding cyclic monomer (or mixtures of both).

The head-to-tail CuAAC reaction has been used in the synthesis of a plethora of cyclic pseudopeptides containing different functionalities. Nilson used the triazole formation to prepare  $C_2$  symmetric macrocyclic/carbohydrate hybrids.<sup>51</sup> Maarseveen reported the synthesis of small peptide analogues that were too strained to yield the cyclic products via macrolactamization.<sup>52</sup> The biological evaluation of a series of cyclotetrapeptide mimics suggests that these analogues retain biological activity when the triazole acts as a *trans* peptide bond isostere.<sup>52b</sup> In a recent example the group of Ghadiri synthesised a series of conformationally homogeneous heterocyclic pseudotetrapeptides that use a triazole linkage as a *trans* peptide bond surrogate and that shows binding to somatostatin receptors.<sup>53</sup> Kubik used a 1,5-disubstituted triazole as a *cis*-amide mimic to modify cyclic pseudopeptides with anion receptor properties.<sup>54</sup> This modification did not affect the overall macrocyclic conformation, leaving the NH inside the cavity to interact efficiently with anions (Figure 9). The modified pseudopeptide showed higher anion affinities in a variety of solvents.

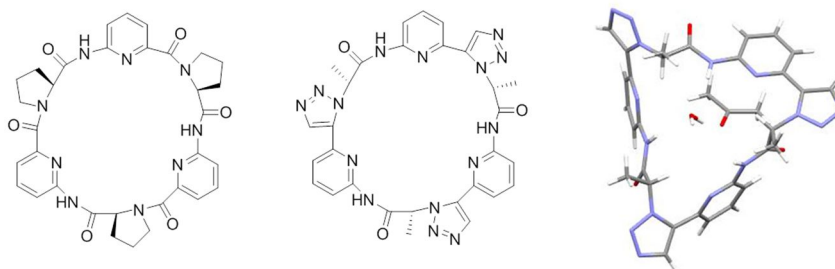
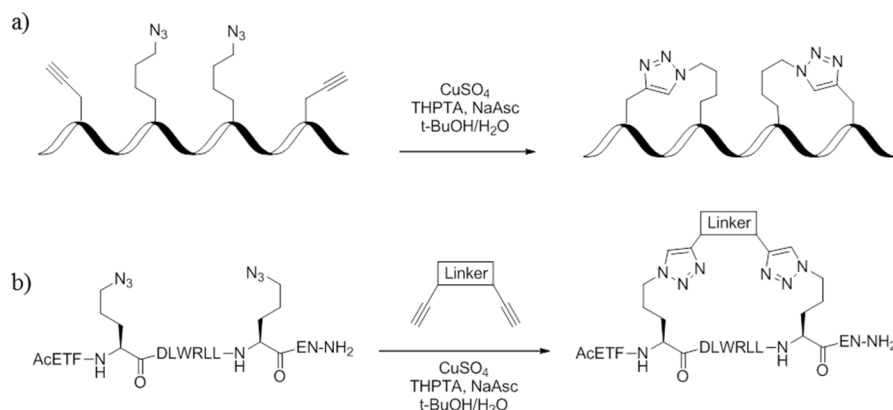


**Figure 9.** Replacement of a *cis*-amide bond by 1,5-disubstituted triazoles in cyclic pseudopeptides developed by Kubik. Left: cyclic peptide developed in the group, right triazole-based peptidomimetic and crystal structure. Cyclic compound crystallized with one molecule of water and one of acetone.

Side chain cyclization has also been extensively reported and it can be performed in the free fully deprotected peptide or with the precursor bound to the resin.<sup>55</sup> Suga incorporated nonproteinogenic amino acids in a ribosomal synthesis that allowed two orthogonal cyclizations. First a chloroacetyl and sulphhydryl group generates the first macrocycle followed by azide-alkyne cyclization.<sup>56</sup> Liskamp also employed the Cu and Ru catalysed click cycloadditions to synthesise new macrocycles inspired in the vancomycin antibiotic.<sup>57</sup> Interestingly, Naismith has very recently reported the enzymatic macrocyclization of triazole-

containing peptidomimetics with one, two or three triazole rings in the peptidic sequence.<sup>58</sup> It is worth mentioning that linking side chains to form a macrocycle is a convenient strategy to stabilize helical conformations; in this context the CuAAC cyclization again provides an easy methodology compatible with most peptidic residues. Thus, Chorev described the preparation and conformational analysis of a peptidomimetic where *i* and *i*+4 side chains were linked by an azide-alkyne cycloaddition constraining the pseudopeptide into an  $\alpha$ -helix conformation.<sup>59</sup> Later, Whang reported a double click reaction to stabilise the conformation on helical peptides, which showed a manifest increase in helical character (Scheme 10a).<sup>60</sup> The resulting 'double staple' is favoured in front of the 'mixed staple'. A different strategy was used by Spring to realize a double-click reaction to generate a peptide staple.<sup>61</sup> In this case the authors reported the use of a terminal bis-acetylene linker to 'click' two azides to stabilise the helical conformation by the formation of a constrained macrocycle (Scheme 10b).



**Scheme 10.** a) Double staple described by Whang's group. b) Double click staple with the introduction of a terminal bis-acetylene linker described by the group of Spring.

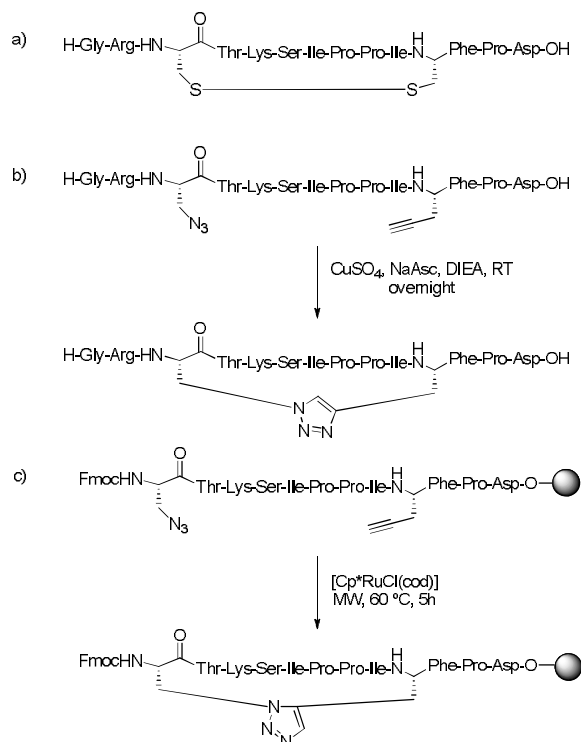
Finally, the triazole unit has been used in cyclic peptides to replace disulphide bonds: 1,5-disubstituted and 1,4-disubstituted triazoles have been employed for this purpose.<sup>62,63</sup> In both cases it has been demonstrated that the peptide maintains its activity while it provides a redox stable replacement for the disulphide bond which translates into improved pharmacokinetic properties (Scheme 11).

### 4.3. Oligomeric triazolamers

The formation of pure triazole-made oligomers is easily achievable thanks to a convenient azo-transfer reaction that allows converting amino-groups to the corresponding azides.<sup>64</sup> Using this methodology it is possible to replace all the amide bonds by triazole-units using solution or solid-phase based methodologies to generate triazole-based oligomers (triazolamers) as described by the group of Arora.<sup>65</sup> Due to the dipole-dipole interactions between adjacent triazole rings a limited amount of conformations are accessible and unique tridimensional structures are obtained. To minimize these dipole-dipole interactions *anti* conformations are preferred, adopting zig-zag conformations which are similar to a  $\beta$ -strand (Figure 10).

A different synthetic approach was developed by Hughes and co-workers to generate racemic triazolamers using fragments that contain an azide and a silyl-protected acetylene.<sup>66</sup> In this strategy (Scheme 12), the alkyne moiety is masked and liberated after each elongation step. In a more recent work, using chiral  $\beta^3$ -substituted trimethylsilyl-homo-propargyl azides a small set of chiral  $\beta^3$  triazolamers was obtained. These compounds, however, adopted linear conformations lacking any ordered secondary structure.<sup>67</sup>

When quaternary amino acids derivatives are used, the conformational space available is restricted by the Thorpe-Ingold effect. Using the same synthetic strategy as Arora for the generation of oligomers, Solà and co-workers synthesised a series of oligomers based on  $\alpha,\alpha$ -disubstituted aminoalkynes to generate a

series of oligomers.<sup>68</sup>

**Scheme 11.** a) Trypsin inhibitor-I (SFTI-1). b,c) Replacement of the disulphide linkage by 1,4-disubstituted triazole (b) and 1,5-disubstituted triazole (c).

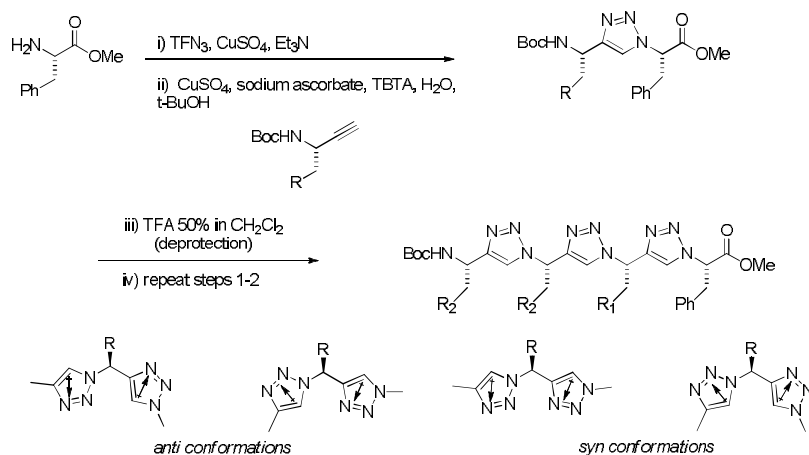
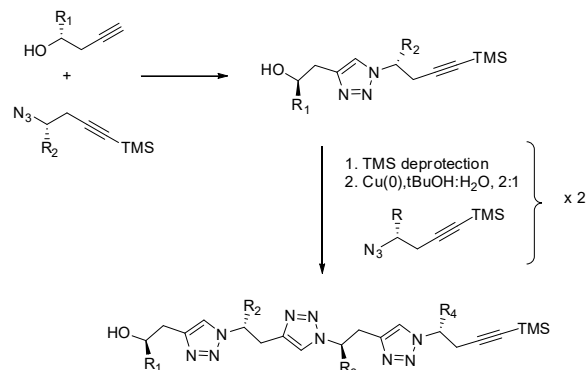


**Figure 10.** a) Arora synthesis of triazolamers. b) Possible *syn*- and *anti*-conformations for contiguous triazoles. According to calculations *anti*-conformations are about 4 kcal/mol more stable than *syn*-conformers.



**Scheme 12.** Synthesis of  $\beta^3$  triazolamers described by Huges and co-workers.

The new synthesised structures presented a similar behaviour to short oligopeptides with different accessible conformations. Thus, planar sheet-structures coexist with twisted strand conformations and the preference for one or the other may be dictated by the presence of hydrogen bond donors or acceptors, the polarity of the solvent, and by the functional groups present in the oligomer (Figure 11). Notably, X-ray diffraction studies on the sheet structure shows different imidazole-C-H $\cdots$ imidazole contacts, which illustrates the ability of imidazoles to establish hydrogen bonds in supramolecular architectures.

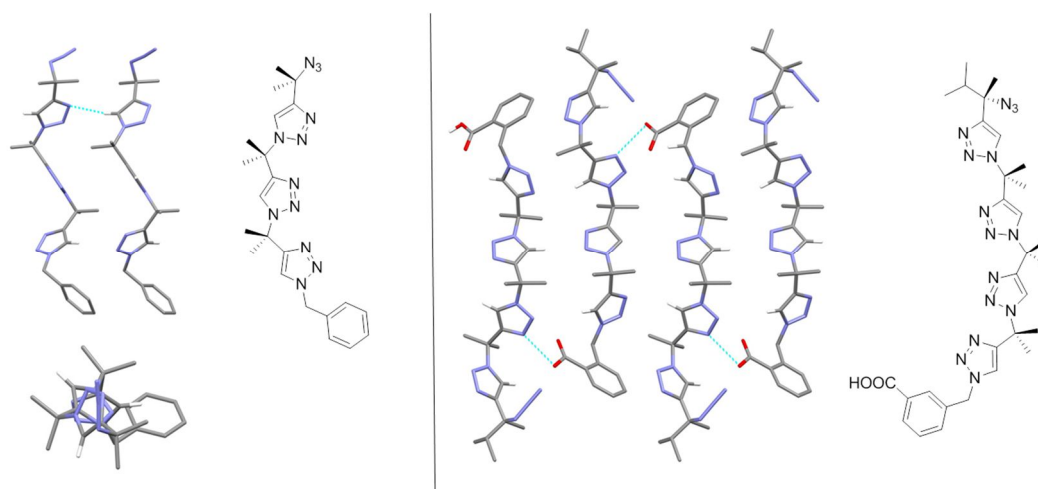


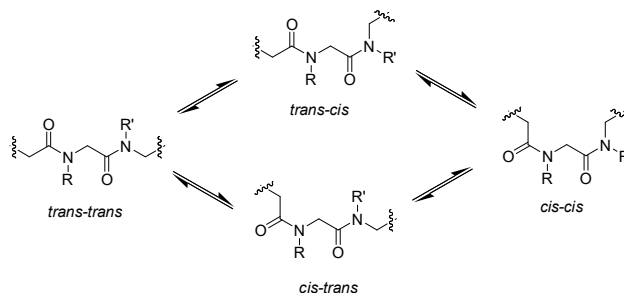
**Figure 11.** Folded (left) and planar zig-zag structures (right) described by Solà and co-workers.

### 5. Disubstituted triazole rings in peptoids

Another group of interesting molecules containing amide bonds as the main function is the general family of peptoids.<sup>69</sup> Peptoids are poly-*N*-alkylglycine oligomers that have been widely used as peptidomimetics in chemical biology, medicinal chemistry and for the development of combinatorial libraries.<sup>70</sup> These molecules contain the tertiary amide as the joint function in the backbone, which also serves for the attachment of the sidechains providing them functional and structural diversity. Moreover, due to the particular conformational properties of tertiary amides, the peptoid chains occupy a large conformational space. Thus, the *cis/trans* amide conformational equilibrium in peptoids is usually slow in the NMR timescale and large populations of the corresponding *cis*-amides are readily visible by <sup>1</sup>H NMR

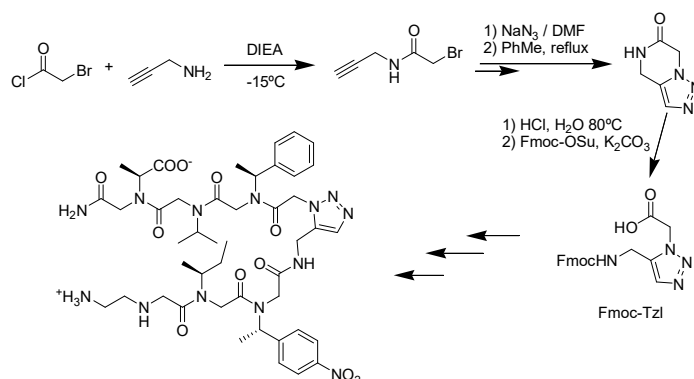


spectral characterization (Scheme 13).<sup>71</sup> As a consequence, in a long peptoid oligomer, a complex mixture of all the possible *cis/trans* amide rotamers is present in solution at room temperature. This structural and conformational diversity is very convenient for identifying hit compounds in the first stage of medicinal chemistry projects, but it is undesired for a hit-to-lead optimization process because a structural heterogeneous peptidomimetic is commonly translated in low selectivity and the appearance of side effects due to off-target interactions.



**Scheme 13.** General structure of a peptoid showing the typical *cis/trans* conformational equilibrium.

For a suitable control of the conformational space around a tertiary amide, the isosteric substitution by a triazole ring has emerged as a very attractive possibility: as previously commented, the *cis/trans* amide bond can be reasonably mimicked by the 1,5- and 1,4-disubstituted triazole ring, respectively. This approach has been exploited by Apella and co-workers in the design of a peptoid oligomer able to fold in a turn conformation in solution.<sup>72</sup> To induce the folded structure, the authors introduced the Tzl amino acid in the middle of the peptoid sequence. This amino acid was easily synthesized from commercial reagents and following an intramolecular thermal Huisgen cycloaddition that was selective toward the 1,5-disubstituted pattern due to the steric hindrance through the formation of a bicyclic intermediate (Scheme 14). The conveniently protected Fmoc-Tzl amino acid was used in conventional peptoid/peptide synthesis to introduce the triazole ring in a peptoid heptamer. The structural studies by CD and NMR showed the turn induction effect of the Tzl moiety, as clearly suggested by control experiments with shorter sequences, the sarcosine mutant and the corresponding 1,4-isomer of Tzl, which all displayed a less defined conformation.



**Scheme 14.** Synthesis of the Tzl amino acid and its incorporation in a turn-folded peptoid.

The use of triazole isomers has been also exploited for the structural and chemical modulation of a cyclic peptoid that was identified as a potent apoptosis inhibitor (Figure 12a).<sup>73</sup> The corresponding cyclic diketopyperazine peptoid identified as an Apaf-1 inhibitor still had an exocyclic tertiary amide that shows

conformational flexibility in terms of cis/trans preferences.<sup>74</sup> Thus, the preparation of isosteres bearing either 1,4- or 1,5-disubstituted triazole rings was envisioned as a way to constrain the side chains in a preferred disposition. Moreover, the 2,4-disubstituted counterpart was also designed as an intermediate conformation.<sup>75</sup> The synthesis of the target molecules was planned by a combination of an Ugi multicomponent reaction followed by a base-promoted intramolecular cyclization reaction (Figure 12b). Unexpectedly, the product of the Ugi reaction undergone cyclization either by the amide nitrogen or through the C $\alpha$  carbon, depending on the triazole substitution pattern and the base used for the cyclization reaction. Thus, both the corresponding diketopyperazine and the  $\beta$ -lactam were obtained, usually as mixtures difficult to separate.

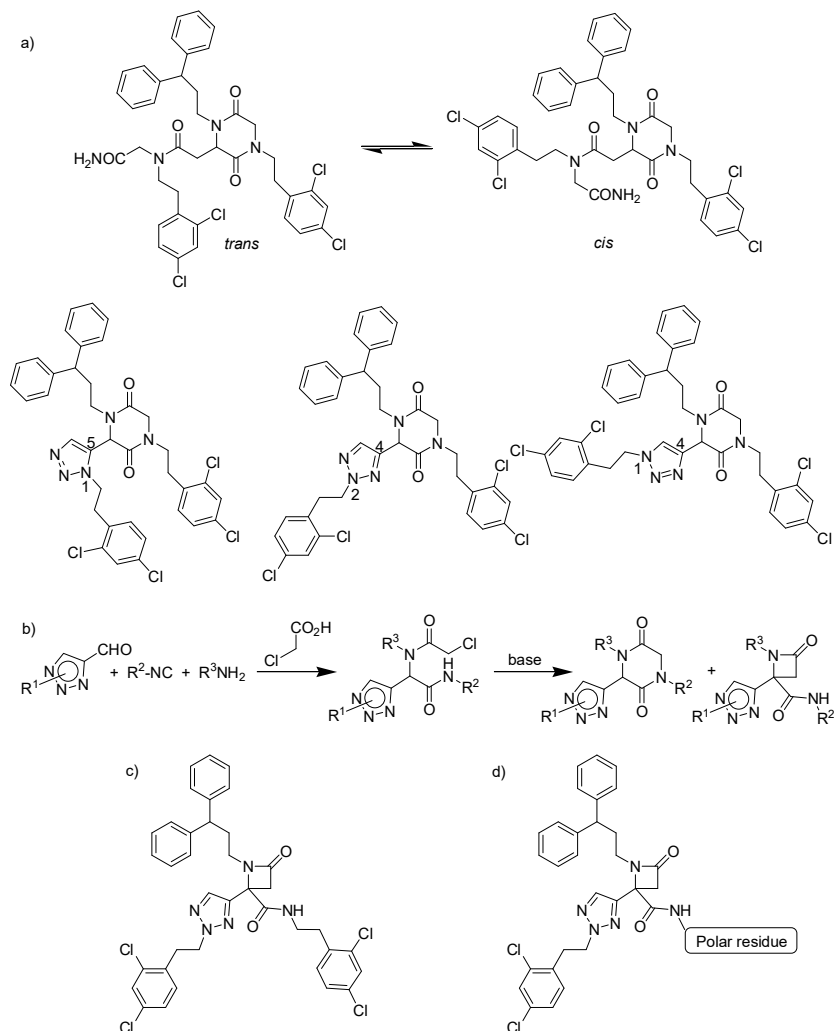


**Figure 12.** a) Conformationally constrained cyclic peptoids with activity as apoptosis inhibitors and proposed triazole isosteres. b) Ugi multicomponent reaction followed by base-promoted cyclization for the synthesis of the constrained triazole peptoids. c) Chemical structure of the most potent Apaf inhibitor. d) Improved derivatives by introduction of polar residues that retains the apoptosis inhibitory activity.

A detailed mechanistic study including theoretical calculations allowed the authors to propose a reasonable explanation for these observations and, more importantly, to optimize the conditions to get good selectivity toward the  $\beta$ -lactams.<sup>76</sup> Very interestingly, biological studies showed the lactams bearing the 2,4-disubstituted triazole as the most potent apoptosis inhibitors (Figure 12c), suggesting that the best conformation for the binding to the target should be an intermediate one between *cis* and *trans* disposition. The same authors further utilized this procedure to design an optimised family of peptidomimetics with improved physicochemical and pharmacological properties, by increasing their aqueous solubility but retaining the apoptosis inhibitory activity (Figure 12d).<sup>77</sup>

## 6. Conclusions

The unique structural and chemical properties of the 1,2,3-triazole ring make this aromatic heterocycle an excellent amide isoster with improved design and stability features. The different substitution within the ring allows better definition of the disposition of the residues attached to the triazole. Moreover, the heterocycle is very stable to biological conditions making it very appealing for biomimetic and biomedical applications. Among the different disubstituted 1,2,3-triazole isomers, the 1,4-substitution has been the most widely used thanks to the very simple and efficient synthesis using the CuAAC reaction. The 1,5-disubstituted isomer can be also obtained by RuAAC reactions although with lower yields and poorer selectivity. The 2,4-derivative is, by far, the less explored isomer although some recent results suggested that it is a very promising candidate in biomedical research. Several structural aspects of these heterocyclic rings, implemented as part of peptides or peptidomimetics allows envisioning a very bright future of this moiety in chemical synthesis and biochemical research.

## Acknowledgements

The financial support from the Spanish Ministry of Economy, Industry and Competitiveness, as well as the European Social Fund (MINECO/FEDER, CTQ2015-70117-R project) and AGAUR (2014 SGR 231) is gratefully acknowledged.

## References

1. a) Gilchrist, T. L. *Heterocyclic Chemistry*, 2<sup>nd</sup> Ed. Longman Scientific & Technical, UK, **1992**. b) Joule, J. A.; Mills, K. *Heterocyclic Chemistry*, 5<sup>th</sup> Ed. John Wiley & Sons, Ltd., Chichester, UK, **2010**.
2. Benson, F. R.; Savell, W. L. *Chem. Rev.* **1950**, *46*, 1-68.
3. Potts, K. T. *Chem. Rev.* **1961**, *61*, 87-127.
4. Peyton, L. R.; Gallagher, S.; Hashemzadeh, M. *Drugs Today (Barc)* **2015**, *51*, 705-718.
5. a) Li, H.; Aneja, R.; Chaiken, I. *Molecules*, **2013**, *18*, 9797-9817. b) Tron, G. C.; Pirali, T.; Billington, R. A.; Canonico, P. L.; Sorba, G.; Genazzani, A. A. *Med. Res. Rev.* **2008**, *28*, 278-308.
6. Angell, Y. L.; Burgess, K. *Chem. Soc. Rev.* **2007**, *36*, 1674-1689.
7. Kolb, H. C.; Finn, M. G.; Sharpless, K. B. *Angew. Chem. Int. Ed.* **2001**, *40*, 2004-2021.
8. Banert, K. *Chem. Ber.* **1989**, *122*, 911-918.
9. Huisgen, R. *Angew. Chem. Int. Ed. Eng.* **1963**, *2*, 633-645.
10. Damodiran, M.; Muralidharan, D.; Perumal, P. T. *Bioorg. Med. Chem. Lett.* **2009**, *19*, 3611-3614.
11. Himo, F.; Lovell, T.; Hilgraf, R.; Rostovtsev, V. V.; Noodleman, L.; Sharpless, K. B.; Fokin, V. V. *J. Am. Chem. Soc.* **2005**, *127*, 210-216.
12. Boren, B. C.; Narayan, S.; Rasmussen, L. K.; Zhang, L.; Zhao, H.; Lin, Z.; Jia, G.; Fokin, V. V. *J. Am. Chem. Soc.* **2008**, *130*, 8923-8930.
13. Tornøe, C. W.; Christensen, C.; Meldal, M. *J. Org. Chem.* **2002**, *67*, 3057-3064.
14. Rostovtsev, V. V.; Green, L. G.; Fokin, V. V.; Sharpless, K. B. *Angew. Chem. Int. Ed.* **2002**, *41*, 2596-2599.
15. Kolb, H. C.; Sharpless, K. B. *Drug Discov. Today* **2003**, *8*, 1128-1137.
16. a) Link, A. J.; Tirrell, D. A. *J. Am. Chem. Soc.* **2003**, *125*, 11164-11165. b) Wang, Q.; Chan, T. R.; Hilgraf, R.; Fokin, V. V.; Sharpless, K. B.; Finn, M. G. *J. Am. Chem. Soc.* **2003**, *125*, 3192-3193.

17. a) Hawker, C. J.; Fokin, V. V.; Finn, M. G.; Sharpless, K. B. *Aust. J. Chem.* **2007**, *60*, 381-383. b) Evans, R. A. *Aust. J. Chem.* **2007**, *60*, 384-395.
18. a) Zhou, Z.; Fahrni, C. J. *J. Am. Chem. Soc.* **2004**, *126*, 8862-8863. b) Lewis, W. G.; Magallon, F. G.; Fokin, V. V.; Finn, M. G. *J. Am. Chem. Soc.* **2004**, *126*, 9152-9153.
19. a) Aucagne, V.; Hanni, K. D.; Leigh, D. A.; Lusby, P. J.; Walker, D. B. *J. Am. Chem. Soc.* **2006**, *128*, 2186-2187. b) O'Reilly, R. K.; Joralemon, M. J.; Hawker, C. J.; Wooley, K. L. *J. Polym. Sci. Polym. Chem.* **2006**, *44*, 5203-5217. c) Zhang, W. B.; Tu, Y.; Ranjan, R.; Van Horn, R. M.; Leng, S.; Wang, J.; Polce, M. J.; Wesdemiotis, C.; Quirk, R. P.; Newkome, G. R.; Cheng, S. Z. D. *Macromolecules* **2008**, *41*, 515-517.
20. Krasinski, A.; Fokin, V. V.; Sharpless, K. B. *Org. Lett.* **2004**, *6*, 1237-1240.
21. a) Tam, A.; Arnold, U.; Soellner, M. B.; Raines, R. T. *J. Am. Chem. Soc.* **2007**, *129*, 12670-12671. b) Imperio, D.; Pilari, T.; Galli, U.; Pagliai, F.; Cafici, L.; Canonico, P. L.; Sorba, G.; Genazzani, A. A.; Tron, G. C. *Bioorg. Med. Chem.* **2007**, *15*, 6748-6757.
22. Zhang, L.; Chen, X.; Xue, P.; Sun, H. H.; Williams, I. D.; Sharpless, K. B.; Fokin, V. V.; Jia, G. *J. Am. Chem. Soc.* **2005**, *127*, 15998-15999.
23. Moumné, R.; Larue, V.; Seijo, B.; Lecourt, T.; Micouin, L.; Tisné, C. *Org. Biomol. Chem.* **2010**, *8*, 1154-1159.
24. Majireck, M. M.; Weinreb, S. M. *J. Org. Chem.* **2006**, *71*, 8680-8683.
25. Krivopalov, V. P.; Shkurko, O. P. *Russ. Chem. Rev.* **2005**, *74*, 339-379.
26. Kamijo, S.; Jin T.; Huo, Z.; Yamamoto, Y. *J. Am. Chem. Soc.* **2003**, *125*, 7786-7787.
27. Kalisiak, J.; Sharpless, K. B.; Fokin, V. V. *Org. Lett.* **2008**, *10*, 3171-3174.
28. a) Rasmussen, L. K.; Boren, B. C.; Fokin, V. V. *Org. Lett.* **2007**, *9*, 5337-5339. b) Johansson, J. R.; Lincoln, P.; Nordén, B.; Kann, N. *J. Org. Chem.* **2011**, *76*, 2355-2359.
29. Holzer, W. *Tetrahedron* **1991**, *47*, 9783-9792.
30. Cohrt, A. E.; Jensen, J. F.; Nielsen, T. E. *Org. Lett.* **2010**, *12*, 5414-5417.
31. Nulwala, H.; Takizawa, K.; Odukale, A.; Khan, A.; Thibault, R. J.; Taft, B. R.; Lipshutz, B. H.; Hawker, C. J. *Macromolecules* **2009**, *42*, 6068-6074.
32. Creary, X.; Anderson, A.; Brophy, C.; Crowell, F.; Funk, Z. *J. Org. Chem.* **2012**, *77*, 8756-8761.
33. Corredor, M.; Bujons, J.; Messeguer, A.; Alfonso, I. *Org. Biomol. Chem.* **2013**, *11*, 7318-7325.
34. For reviews on triazole-based peptidomimetics see ref 6 and a) Holub, J. M.; Kirshenbaum, K. *Chem. Soc. Rev.* **2010**, *39*, 1325-1337. b) Pedersen, D. S.; Abell A. D. *The Huisgen cycloaddition in peptidomimetic chemistry in: Amino Acids, Peptides and Proteins in Organic Chemistry*. Wiley-VCH, Weinheim, Germany, **2011**.
35. Zabrocki, J.; Smith, G. D.; Dunbar, J. B. Jr.; Iijima, H.; Marshall, G. R. *J. Am. Chem. Soc.* **1988**, *110*, 5875-5880.
36. Tornøe, C. W.; Sanderson, S. J.; Mottram, J. C.; Coombs, G. H.; Meldal, M. *J. Comb. Chem.*, **2004**, *6*, 312-324.
37. Zhang, Z.; Fan, E. *Tetrahedron Lett.* **2006**, *47*, 665-669.
38. a) Horne, W. S.; Stout, C. D.; Ghadiri, M. R. *J. Am. Chem. Soc.* **2003**, *125*, 9372-9376. b) van Maarseveen, J. H.; Horne, W. S.; Ghadiri, M. R. *Org. Lett.* **2006**, *7*, 4503-4506.
39. Horne, W. S.; Yadav, M. K.; Stout, C. D.; Ghadiri, M. R. *J. Am. Chem. Soc.* **2004**, *126*, 15366-15367.
40. Brik, A.; Alexandratos, J.; Lin, Y. C.; Elder, J. H.; Olson, A. J.; Wlodawer, A.; Goodsell, D. S.; Wong, C. H. *ChemBioChem*, **2005**, *6*, 1167-1169.
41. Whiting, M.; Muldoon, J.; Lin, Y. C.; Silverman, S. M.; Lindstrom, W.; Olson, A. J.; Kolb, H. C.; Finn, M. G.; Sharpless, K. B.; Elder, J. H.; Fokin, V. V. *Angew. Chem. Int. Ed.* **2006**, *45*, 1435-1439.
42. Tischler, M.; Nasu, D.; Empting, M.; Schmelz, S.; Heinz, D. W.; Rottmann, P.; Kolmar, H.; Buntkowsky, G.; Tietze, D.; Avrutina, O. *Angew. Chem. Int. Ed.* **2012**, *51*, 3708-3712.
43. a) Valverde, I. E.; Bauman, A.; Kluba, C. A.; Vomstein, S.; Mindt, T. L. *Angew. Chem. Int. Ed.* **2013**, *52*, 8957-8960. b) Valverde, I. E.; Vomstein, S.; Fischer, C. A.; Mascarín, A.; Mindt, T. L. *J. Med. Chem.* **2015**, *58*, 7475-7484.
44. Hartwig, S.; Hecht, S. *Macromolecules*, **2010**, *43*, 242-248.
45. Ke, Z.; Chow, H.-F.; Chan, M.-C.; Liu, Z.; Sze, K.-H. *Org. Lett.* **2012**, *14*, 394-397.

46. Johansson, J. R.; Hermansson, E.; Nordén, B.; Kann, N.; Beke-Somfai, T. *Eur. J. Org. Chem.* **2014**, 2703-2713.
47. Kann, N.; Johansson, J. R.; Beke-Somfai, T. *Org. Biomol. Chem.* **2015**, *13*, 2776-2785.
48. White, C. J.; Yudin, A. K. *Nature. Chem.* **2011**, *3*, 509-524.
49. a) Ghorai, A.; Gayen, A.; Kulsi, G.; Padmanaban, E.; Laskar, A.; Achari, B.; Mukhopadhyay, B.; Chattopadhyay, P. *Org. Lett.* **2011**, *13*, 5512-5515. b) Ghorai, A.; Padmanaban, E.; Mukhopadhyay, C.; Achari, B.; Chattopadhyay, P. *Chem. Commun.* **2012**, *48*, 11975-11977. c) Kulsi, G.; Ghorai, A.; Achari, B.; Chattopadhyay, P. *RSC Adv.* **2015**, *5*, 64675-64681.
50. Jagasia, R.; Holub, J. M.; Bollinger, M.; Kirshenbaum, K.; Finn, M. G. *J. Org. Chem.* **2009**, *74*, 2964-2974.
51. Billing, J. F.; Nilsson, U. J. *J. Org. Chem.* **2005**, *70*, 4847-4850.
52. a) Bock, V. D.; Perciaccante, R.; Jansen, T. P.; Hiemstra, H.; van Maarseveen, J. H. *Org. Lett.* **2006**, *8*, 919-922. b) Bock, V. D.; Speijer, D.; Hiemstra, H.; van Maarseveen, J. H. *Org. Biomol. Chem.* **2007**, *5*, 971-975.
53. Beierle, J. M.; Horne, W. S.; van Maarseveen, J. H.; Waser, B.; Reubi, J. C.; Ghadiri, M. R. *Angew. Chem. Int. Ed.* **2009**, *48*, 4725-4729.
54. Krause, M. R.; Goddard, R.; Kubik, S. *J. Org. Chem.* **2011**, *76*, 7084-7095.
55. Roice, M.; Johannsen, I.; Meldal, M. *Qsar. Comb. Sci.* **2004**, *23*, 662-673.
56. Sako, Y.; Morimoto, J.; Murakami, H.; Suga, H. *J. Am. Chem. Soc.* **2008**, *130*, 7232-7234.
57. a) Zhang, J.; Kemmink, J.; Rijkers, D. T. S.; Liskamp, R. M. J. *Org. Lett.* **2011**, *13*, 3438-3441. b) Zhang, J.; Kemmink, J.; Rijkers, D. T. S.; Liskamp, R. M. J. *Chem. Commun.* **2013**, *49*, 4498-4500.
58. Oueis, E.; Jaspars, M.; Westwood, N. J.; Naismith, J. H. *Angew. Chem. Int. Ed.* **2016**, *55*, 5842-5845.
59. Cantel, S.; Isaad, A. C.; Scrima, M.; Levy, J. J.; DiMarchi, R. D.; Rovero, P.; Halperin, J. A.; D'Ursi, A. M.; Papini, A. M.; Chorev, M. *J. Org. Chem.* **2008**, *73*, 5663-5674.
60. Kawamoto, S. A.; Coleska, A.; Ran, X.; Yi, H.; Yang, C.-Y.; Wang, S. *J. Med. Chem.* **2012**, *55*, 1137-1146.
61. a) Lau, Y. H.; de Andrade, P.; Sköld, N.; McKenzie, G. J.; Venkitaraman, A. R.; Verma, C.; Lane, D. P.; Spring, D. R. *Org. Biomol. Chem.* **2014**, *12*, 4074-4077. b) Lau, Y. H.; Wu, Y.; de Andrade, P.; Galloway, W. R. J. D.; Spring, D. R. *Nat. Protoc.* **2015**, *10*, 585-594.
62. Empting, M.; Avrutina, O.; Meusinger, R.; Fabritz, S.; Reinwarth, M.; Biesalski, M.; Voigt, S.; Buntkowsky, G.; Kolmar, H. *Angew. Chem. Int. Ed.* **2011**, *50*, 5207-5211.
63. Holland-Nell, K.; Meldal, M. *Angew. Chem. Int. Ed.* **2011**, *50*, 5204-5206.
64. a) Alper, P. B.; Hung, S.-C.; Wong, C.-H. *Tetrahedron Lett.* **1996**, *37*, 6029-6032. b) Goddard-Borger, E. D.; Stick, R. V. *Org. Lett.*, **2007**, *9*, 3797-3800.
65. a) Angelo, N. G.; Arora, P. S. *J. Am. Chem. Soc.* **2005**, *127*, 17134-17135. b) Angelo, N. G.; Arora, P. S. *J. Org. Chem.* **2007**, *72*, 7963-7967.
66. Montagnat, O. D.; Lessene, G.; Hughes, A. B. *Tetrahedron Lett.* **2006**, *47*, 6971-6974.
67. Montagnat, O. D.; Lessene, G.; Hughes, A. B. *J. Org. Chem.* **2010**, *75*, 390-398.
68. Solà, J.; Bolte, M.; Alfonso, I. *Org. Biomol. Chem.* **2015**, *13*, 10797-10801.
69. Simon, R. J.; Kania, R. S.; Zuckermann, R. N.; Huebner, V. D.; Jewell, D. A.; Banville, S.; Ng, S.; Wang, L.; Rosenberg, S.; Marlowe, C. K.; Spellmeyer, D. C.; Tan, R.; Frankel, A. D.; Santi, D. V.; Cohen, F. E.; Bartlett, P. A. *Proc. Natl. Acad. Sci. U.S.A.* **1992**, *89*, 9367-9371.
70. Miller, S. M.; Simon, R. J.; Ng, S.; Zuckermann, R. N.; Kerr, J. M.; Moos, W. H. *Drug Dev. Res.* **1995**, *35*, 20-32.
71. Sui, Q.; Borchardt, D.; Rabenstein, D. L. *J. Am. Chem. Soc.* **2007**, *129*, 12042-12048.
72. Pokorski, J. K.; Jenkins, L. M. M.; Feng, H.; Durell, S. R.; Bai, Y.; Appella, D. H. *Org. Lett.* **2007**, *9*, 2381-2383.
73. a) Mondragón, L.; Orzáez, M.; Sanclimens, G.; Moure, A.; Armiñán, A.; Sepúlveda, A.; Messeguer, A.; Vicent, M. J.; Pérez-Payá, E. *J. Med. Chem.* **2008**, *51*, 521-529; b) Mondragón, L.; Galluzzi, L.; Mouhamad, S.; Orzáez, M.; Vicencio, J. M.; Vitale, I.; Moure, A.; Messeguer, A.; Pérez-Payá, E.; Kroemer, G. *Apoptosis* **2009**, *14*, 182-190.

74. Moure, A.; Sanclimens, G.; Bujons, J.; Masip, I.; Alvarez-Larena, A.; Pérez-Payá, E.; Alfonso, I.; Messeguer, A. *Chem. Eur. J.* **2011**, *17*, 7927-7939.
75. Corredor, M.; Bujons, J.; Orzáez, M.; Sancho, M.; Pérez-Payá, E.; Alfonso, I.; Messeguer, A. *Eur. J. Med. Chem.* **2013**, *63*, 892-896.
76. Corredor, M.; Garrido, M.; Bujons, J.; Orzáez, M.; Pérez-Payá, E.; Alfonso, I.; Messeguer, A. *Chem. Eur. J.* **2015**, *21*, 14122-14128.
77. Garrido, M.; Corredor, M.; Orzáez, M.; Alfonso, I.; Messeguer, A. *ChemistryOpen* **2016**, *5*, 485-494.